ELSEVIER

Materials Science and Engineering A265 (1999) 100–109

MATERIALS SCIENCE & ENGINEERING A

The effect of off-axis thermomechanical processing on the mechanical behavior of textured 2095 Al–Li alloy

E.W. Lee [a], P.N. Kalu [b], L. Brandao [b,c], O.S. Es-Said [d], J. Foyos [d], H. Garmestani [b,*]

[a] *Code 4.3.4.2, Naval Air Warfare Center, A/C Div., Warminster, PA 18974, USA*
[b] *FAMU-FSU College of Engineering, Department of Mechanical Engineering and Center for Materials Research and Technology (MARTECH), Room 229, 2525 Pottsdamer Road, Tallahassee, FL 32310-6046, USA*
[c] *Departamento de Eng. Mecanica e de Materiais, IME, Rio de Janeiro, RJ 22290-270, Brazil*
[d] *Department of Mechanical Engineering, Loyola Marymount University, Los Angeles, CA 90045-8145, USA*

Received 5 August 1998; received in revised form 30 November 1998

Abstract

This investigation was conducted to study the influence of off-axis deformation in the thermomechanical processing on the properties of Al–Li 2095 HT72 alloy sheet. The thermomechanical processing involved several stages. First, the as-received hot rolled sheet was solution heat treated at 510°C for 30 min. Samples were then cut from the sheet and stretched off-axis at 0, 30, 60 and 90° angles (stretch axis) to the original rolling direction. All the specimens were then aged at 180°C for 24 h. Tensile coupons were then machined from each of these aged samples at 0, 30, 45, 60 and 90° (tensile axis) to the rolling direction, then tested to failure. The crystallographic texture and tensile properties of the processed samples were evaluated, and were compared to the solution heat-treated material. In the solution heat-treated condition, the material was highly textured with a very strong Brass component. Off-axis stretch followed by aging had little or no effect on the texture development of the solution heat-treated material. Upon testing, samples with stretch axis at 0° showed pronounced mechanical anisotropy; specimens tested at 45° showed about 40% drop in tensile and yield strength values when compared to those tested at 0°. However, stretching along 60° or 90° directions minimized mechanical anisotropy. The texture characteristics of all tested samples were determined and related to the changes in the mechanical properties. An attempt was made to correlate the data with some texture theories. Analysis of the results and normalization based on the Taylor's factor showed that that crystallographic texture contributes only partly to the total mechanical anisotropy.

Keywords: Off-axis thermomechanical processing; Mechanical behavior; 2095 Al–Li alloy

1. Introduction

The processing of advanced aluminum alloy sheets by conventional ingot metallurgy (IM) techniques involves casting ingots, hot forging into billets, followed by several hot rolling and heat treatment sequences to produce plates or sheets that are used in subsequent applications. In recent years Al–Li alloys have received considerable attention from both the industrial and scientific communities because of their high modulus/specific strength and low density. These properties are particularly attractive to designers of high performance military and commercial aircraft. Aluminum–Lithium alloys processed through IM casting with subsequent forming operations are currently being developed for aerospace applications [1]. However, commercial Al–Li alloys exhibit tensile strength anisotropy when compared to conventional 2xxx and 7xxx type aerospace alloys. In sheet or plate form, mechanical property anisotropy is manifested on the rolling plane. Thermomechanical treatments such as rolling and stretching have been employed to improve the overall mechanical properties of these alloys. Using these techniques, highly textured sheet metals with pronounced mechanical anisotropy are produced which may not be desirable for some industrial applications [2]. The mechanical properties of these materials depend on the direction in which they are measured, and this phenomenon may be

* Corresponding author. Tel.: +1-850-6445993; fax: +1-850-6449281.
E-mail address: garm@magnet.fsu.edu (H. Garmestani)

0921-5093/99/$ - see front matter
PII: S0921-5093(98)01150-2

attributed to the crystallographic texture, grain shape and morphology [3,4]. Recently, Es-Said and Lee [5] have reported success in reducing mechanical anisotropy of 2095 Al–Li sheets produced by conventional techniques via the incorporation of off-axis rolling/stretching prior to aging.

While the microstructures and mechanical properties of IM aluminum alloys have been extensively characterized, the correlation of microstructure and texture is still a subject of current interest [6]. The effect of precipitates on anisotropy has also been investigated in a number of Al–Li alloys in recent years [3,7,8]. The role of preferentially oriented precipitates in inducing mechanical anisotropy cannot be over emphasized [8–10]. What is not fully understood is the effect of precipitates on crystallographic texture and the resulting anisotropy [4,11,12].

Depending on the alloying elements and processing conditions different types of precipitates exist in aluminum [13]. The $\delta'(Al_3Li)$ and $\delta(AlLi)$ phases are the common phases formed through precipitation in Al–Li based alloys, whereas $\theta'(Al_2Cu)$ and $T_1(Al_2CuLi)$ are the reported precipitation phases for Al–Li-Cu alloys [1]. The T_1 phase is the major source of strengthening in Al–Li-Cu alloys [14,15]. This precipitate has a hexagonal structure, and occurs as plates on {111}—a major slip plane for face-centered cubic alloys. In the work by Kim and Lee [8] the effect of T_1 precipitate on the anisotropy of an Al–Li alloy 2090 was investigated. It was shown that there is an inhomogeneous distribution of $T_1(Al_2CuLi)$ plate-shaped precipitates among the four {111} habit planes after stretching and aging of a 2090 aluminum lithium alloy. It was further reported that this inhomogeneous distribution of T_1 precipitates has a direct effect on the mechanical anisotropy of the material. When samples were pulled at orientations parallel to the rolling direction, a high density of T_1 precipitates intercepted the active slip plane. This resulted in homogeneous deformation. However, when the samples were pulled at 60° orientation with respect to the rolling direction, a low density of precipitates was developed. The density of T_1 precipitates so produced was insufficient to influence the deformation behavior of the material.

The micromechanics of such a process is still not well understood and most of the past work in this area has been concerned with correlating properties with precipitate size or spacing [16]. The full understanding of this process requires experiments and modeling efforts to relate crystallographic texture, anisotropy and the inhomogeneous distribution of precipitates. It is also desirable to isolate the effect of texture and understand the mechanism of deformation and dislocation–precipitation interaction. In the present work, the effect of off-axis deformation on mechanical properties and crystallographic textures in 2095 HT72 Al–Li alloy has been investigated. Also, an attempt was made to explain the influence of texture on the mechanical anisotropy using the upper bound method. Both restricted glide and pencil glide approaches were considered. Our analysis had to take into account the effect of T_1 precipitates during deformation, since the microstructural development of Al–Li alloys deformed by off-axis stretching and rolling is heavily influenced by the presence of T_1 precipitates [8].

2. Experimental procedure

The nominal composition of the 2095 HT72 aluminum–lithium alloy used in this investigation is presented in Table 1. The material was received as hot rolled sheets (1.57 mm thickness), and then solution heat treated at 510°C for 30 min. Samples were cut from the sheet and stretched 6% off-axis at 0, 30, 60 and 90° angles (stretch axis (SA)) to the rolling direction. The samples are thereafter identified as S0, S6 and S9, respectively. A schematic showing the stretch and machining orientations of the samples is presented in Fig. 1. The specimens were then aged at 180°C for 24 h. Tensile coupons were machined from aged samples at 0, 30, 45, 60 and 90° angles (tensile axis (TA)) to the original hot rolling direction. The tensile coupons machined from the stretched samples are identified as: S00, S03,…; S60, S63, …; and S90, S93, …. Coupons machined from the rolled samples are R40, R43, R44, R46 and R49. A flowchart showing the sequence of processing and the sample identifications at each stage of processing is presented in Fig. 2. The sample identifications used are such that the first number indicates the first digit of the SA and the second number indicates the first digit of the TA. The machined specimens were tested in tension at a constant cross-head speed of 1.27 mm min^{-1}. The schematic diagrams showing the tensile coupons for the 60° and 90° stretched samples are shown in Fig. 3(a, b), respectively. Three coupons were tested at each test condition, hence, each data point represents the mean of three tests.

Specimens for texture analysis were cut from the materials, mechanically polished, and etched to remove any residual deformation layers. In all cases, the original rolling direction was used as the pole figure reference direction. The crystallographic texture was evaluated using the X-ray diffraction technique on a

Table 1
Chemical compositions of 2095 HT72 aluminum–lithium alloy investigated

	Cu	Li	Mg	Zr	Ag
2095	3.9–4.6	1.0–1.6	0.25–0.8	0.04–0.18	0.25–0.6

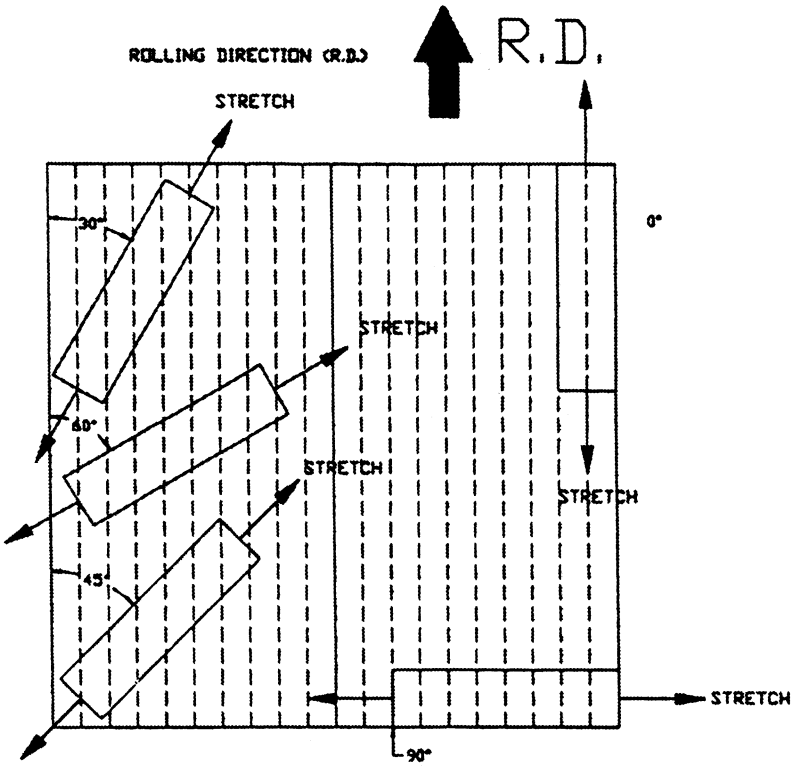

Fig. 1. Stretch orientation in relation to the hot rolling direction.

Philips X'Pert PW3040 MRD X-ray diffractometer operating at 40 kV and 50 mA using CuK_{α} radiation. The diffractometer was equipped with a curve monochromator. Three incomplete pole figures (111), (200), and (220) were obtained using the reflection technique. The resulting data was analyzed using the popLA software package [17] from which the Orientation Distribution Functions (ODFs) were calculated using the spherical harmonic approach. In order to evaluate the texture effect on mechanical anisotropy, Taylor factor 'M' was calculated directly from the harmonic coefficients of the ODF using popLA software package [17] for two different conditions: restricted glide (RG) and pencil glide (PG).

3. Results

3.1. Texture

3.1.1. Solution heat treated material

The ODF sections at $\phi = 0°$ and 45° for the solution heat-treated material is presented in Fig. 4. As expected, the material exhibited typical FCC rolling texture with a strong Brass $\{110\}<112>$ and a weak Copper $\{112\}<111>$ component, with intensity values of about 40 × and 2 × random, respectively. Other strong texture components observed included P $\{110\}<122>$, S $\{123\}<634>$ and shear $\{111\}<112>$ orientations, with intensity of about 10 × random. Some of the weak texture components observed were Goss $\{110\}<001>$, X $\{110\}<111>$, R $\{124\}<211>$, transverse direction rotated Cube (RCT) $\{013\}<013>$, and normal direction rotated Cube (RCN) $\{001\}<013>$ orientations.

A very high Brass intensity, such as seen in this material is not uncommon with Al–Li alloys, especially in Al–Li superplastic materials [18]. The TD rotated cube texture is formed by 20° rotation of the Cube orientation about the transverse direction. This component is classified as a recrystallization texture, and may have been formed during the hot rolling process performed on the material. Two components of $\{111\}<110>$ and $\{111\}<112>$ shear orientations are also observed and referred to as Sh1 and Sh2 respectively. The $\{111\}<112>$ shear component (Sh2) has the $\{111\}$ planes parallel to the rolling plane and has been observed in some Al alloys deformed under certain deformation conditions [7,19,20]. For example, Al alloy deformed in torsion was characterized by this shear component [21]. Also, Al-2195 alloy processed by rollring forging exhibited $\{111\}<112>$ along with other shear components [20]. The mechanism for the formation of $\{111\}<112>$ shear may involve the rotation of some or all $\{112\}<111>$ and $\{001\}<110>$ components about the transverse direction to $\{554\}<225>$—an orientation close to $\{111\}<112>$ [20]. This will explain the low intensity observed for these two components.

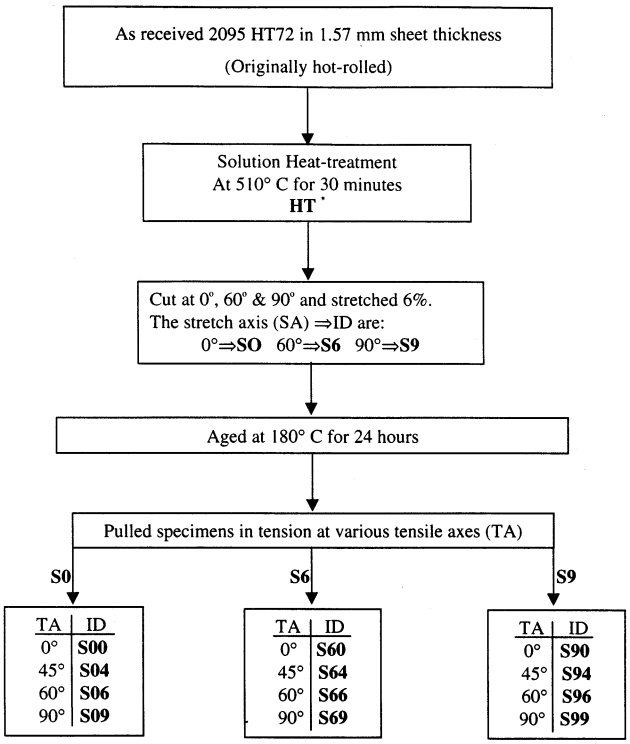

Fig. 2. The flow chart of the thermomechanical processing condition. *Bold face represent specimen identification.

3.1.2. Effect of off-axis stretch accompanied by aging

As stated in the experimental section, following solution heat treatment, the materials were cut at various orientations and given a 6% stretch, then aged. Fig. 5(a–c) present the ODF sections at $\phi = 0°$ and 45° for materials with SA at 0°, 60° and 90°, respectively. Qualitatively, the texture components present in these three materials were similar and comparable to that observed for the solution heat-treated material. Summary of the deformation and recrystallization texture components found in these materials are shown in Fig. 6(a, b), respectively. The intensity difference of the principal texture components in these materials was within 15%. It is therefore reasonable to conclude that the off-axis deformation (stretch) plus aging heat treatment had little or no effect on the texture of the solution heat-treated material. This result is not surprising in light of the small strain (6% stretch) and the low aging temperature of 180°C used in the processing. With such low aging temperature, the material is not expected to undergo recrystallization. However, a limited amount of recovery may occur, and this will not cause any dramatic change in texture.

3.1.3. Effect of tensile deformation

After aging, the materials were tested in tension until failure at various orientations resulting in additional strains of up to 12% in some off-axis orientation. These initial orientations are denoted as the TA. The texture components in the tested materials have been compared with those of the solution heat treated/aged materials, and the summary is presented in Figs. 7–9. This summary is based on repeated tests on a number of samples (at least three) and also repeated number of pole figure analysis. In Fig. 7, the intensities of the texture compo-

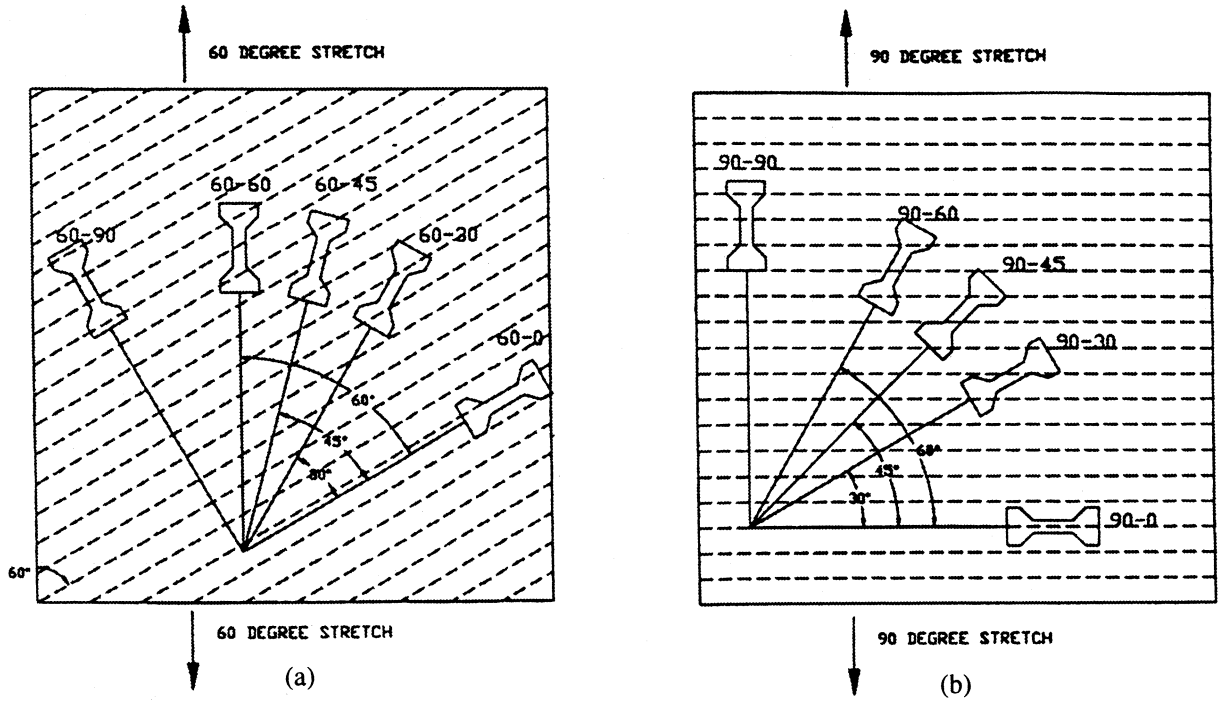

Fig. 3. Machine orientation of the tensile coupons. Samples in 60° stretch (a) and 90° stretch (b).

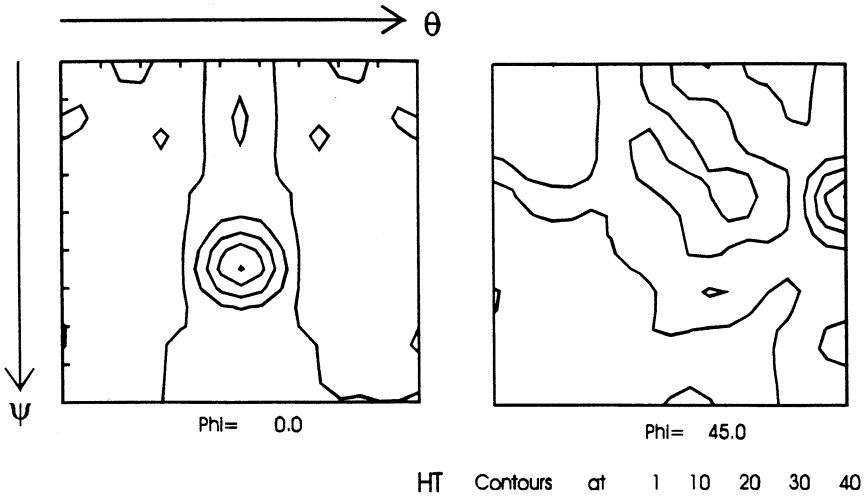

Fig. 4. ODF sections for the solution heat treated 2095 alloy.

nents of the deformed specimens were comparable to the solution heat-treated material except for the S04 sample (sample with SA = 0° and TA = 45°). In this case, the Brass, Copper, S, shear and R components disappeared, while the X component was increased. It is interesting to note that the texture of the material with SA = 60° was comparable to the solution heat-treated material, regardless of the tensile axis (Fig. 8). For the material with SA = 90°, the R and S components increased with a corresponding decrease in Brass component, when the TA = 45° (Fig. 9).

3.2. Mechanical properties

3.2.1. Effect of off-axis stretch

The effect of varying the orientation of the 6% stretching prior to aging on the tensile properties is shown in Fig. 10(a–c) [5]. In the zero degree stretch (parallel to the rolling direction), the tensile strength drops 25–40%, when the angle between the tensile axis and the rolling direction is 45°. These results are in accordance with the findings of Lee and Waldman [22], and Lee and Frazier [12]. At 0° with respect to rolling direction, high tensile strength, uniform elongation and uniform distribution of dislocations were observed, [22]; at 45–60° to the rolling direction, 15–20% lower strength, non-uniform elongation and localized slip were observed. The localized deformation was attributed to the inhomogeneous distribution of the T_1 precipitation among the four {111} habit planes [8]. The tensile strength drops 10–12% when the angle is 45° for the 60° stretch and 10–15% when the angle is 45–60° for the 90° stretch (Fig. 10(b, c)). The tensile yield and ultimate strengths in the 90° stretch exceeded 553 and 587 MPa, respectively, in all orientations. These values are superior to the corresponding strengths of the 7075-T6 aluminum alloys [22].

The elongation to failure was also highly anisotropic (Fig. 11). This means that the off-axis stretched specimens have been exposed to different strain levels once they were deformed to failure in different directions. In the case of the 90° stretch the difference in strains between the 0 and 90° samples was as high as 9%. In general the specimens oriented at 45° were strained twice the samples which were oriented at 0°. This may partially explain the minimal differences in texture as is evident in Figs. 6–9.

4. Discussion

An attempt has been made in this investigation to evaluate the influence of off-axis thermomechanical processing on mechanical properties and crystallographic texture of Al–Li 2095 material. It is well known that in a single-phase material, the plastic anisotropy depends mainly on its crystallographic texture. It is also well established that texture is a function of the thermomechanical history of a material. In view of the fact that Al–Li 2095 alloy contains several precipitates, which influence the thermomechanical history of the material, the reported results cannot be explained only in the light of crystallographic texture. The principal strengthening precipitate in high lithium containing alloys is $T_1(Al_2CuLi)$ [14]. However, other precipitates such as $\theta'(Al_2Cu)$ and $S'(Al_2CuMg)$ have also been observed in artificially aged high copper high lithium alloys [23,24]. It is therefore important to have a separate discussion of the contribution of the T_1 precipitates and the texture on plastic anisotropy of the Al–Li 2095 HT72 alloy.

As shown in Section 3.1.2., the variation in texture of the materials subjected to stretching (alone) at various axis was insignificant. This demonstrates that the off-

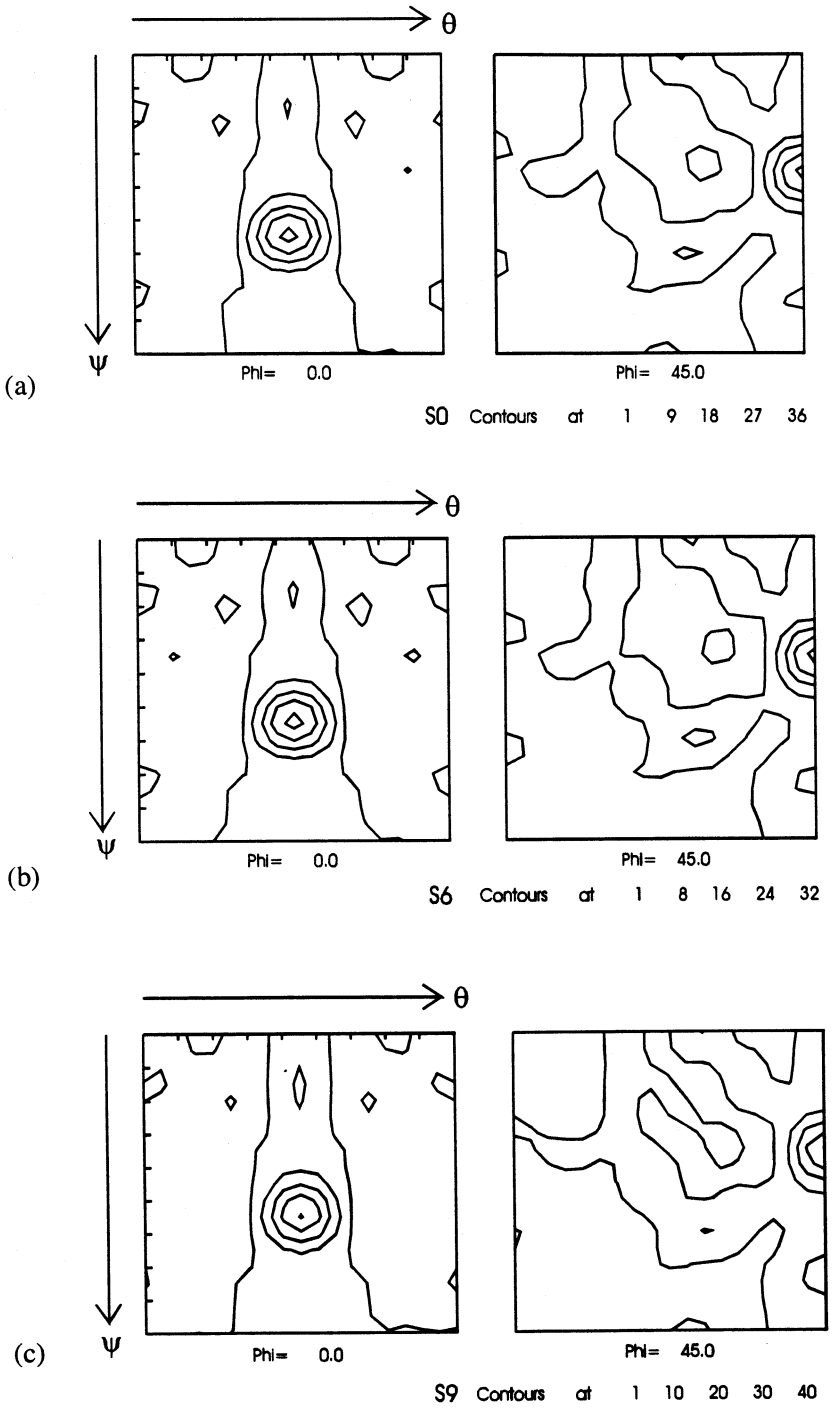

Fig. 5. ODF sections for the stretched and aged material conditions (a) S0, (b) S6 and (c) S9.

axis stretching alone had little or no effect on the crystallographic texture of the Al–Li 2095 HT72. Therefore, all the stretched materials used for tensile testing started with essentially a similar texture. A comparison of the results presented in Fig. 10(a–c) show that the yield strength anisotropy was different for the various stretch conditions. This result indicates that texture alone cannot be used to explain all the differences in the mechanical properties. Kumar et al. [24] showed that stretching prior to aging plays an important role in the precipitation of T_1 and S′ phases. Kim and Lee [8] found inhomogeneous distribution of T_1 precipitates on {111} planes, with a corresponding strong $\{110\}<112>$ texture in Al–Li 2090 alloy. They also correlated the inhomogeneous distribution of T_1 precipitates on the slip planes and tensile properties, especially elongation. Kim and Lee [8] attributed the difference in mechanical anisotropy observed essentially

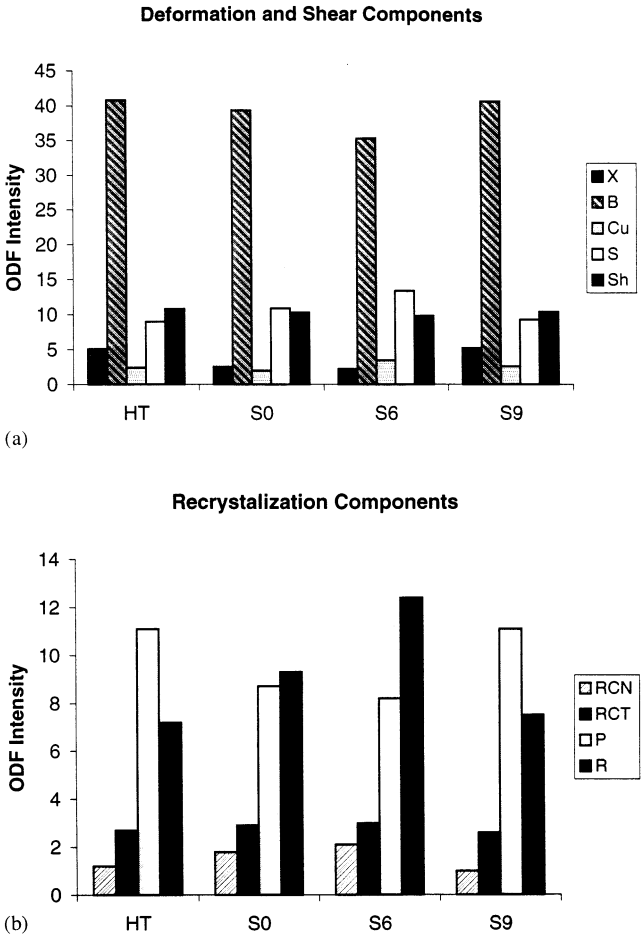

Fig. 6. Comparison of texture components of solution heat treated and aged materials, (a) principal deformation and shear components and (b) main recrystallization components.

to the precipitates and showed that crystallographic texture alone cannot explain the apparent anisotropy. That analysis used a normalization technique comparing the highly textured material to a single crystal with $\{110\}<112>$ orientation. As a result the mechanical

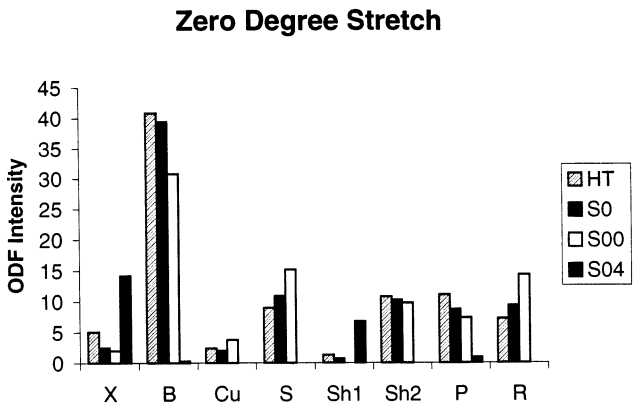

Fig. 7. Comparison of main texture components of solution heat treated material and aged samples stretched at 0° after mechanical testing.

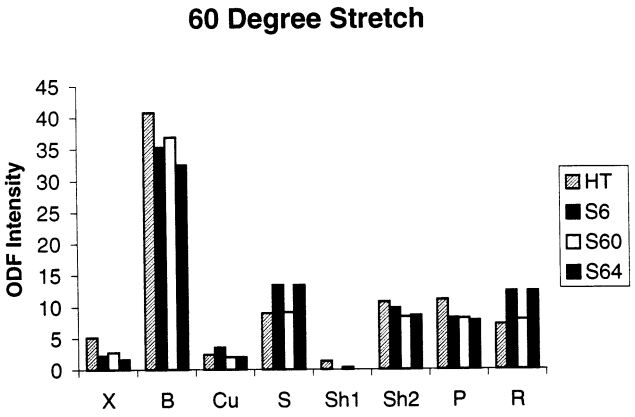

Fig. 8. Comparison of main texture components of solution heat treated material and aged samples stretched at 60° after mechanical testing.

properties were normalized using the Schmid factor. The present investigation performs the same normalization using the Taylor's factor calculated from the texture analysis. Taylor Factor 'M' is used as the orientation factor and denotes the effect of texture on the mechanical properties, especially on the yield strength and ultimate tensile strength. The values of 'M' were calculated from the harmonic coefficients of the ODF based on RG and are presented in Table 2. The predictions were made using the harmonic coefficients of the ODF of the stretched and subsequently aged materials and then deformed at various tensile axes (TA) [16].

In the restricted glide, the dislocation can only move on the slip system, where, both the slip plane and direction are close-packed. This has been effectively used to explain deformation in FCC materials, where the slip system is $\{111\}<110>$. Although the restricted glide approach is always applied to FCC material, there have been reports of non-octahedral slip in aluminum alloys [9,16,25,26]. Maurice et al. [25]

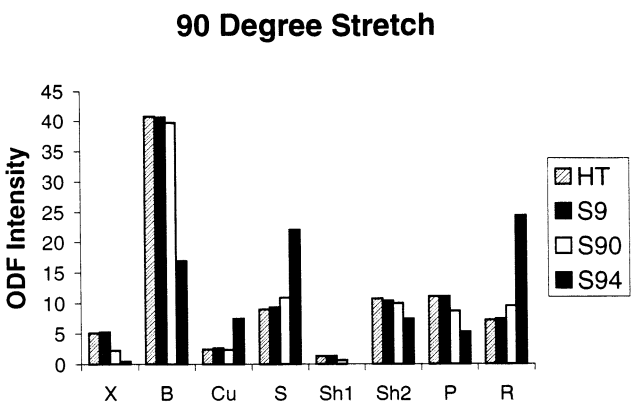

Fig. 9. Comparison of main texture components of solution heat treated material and aged samples stretched at 90° after mechanical testing.

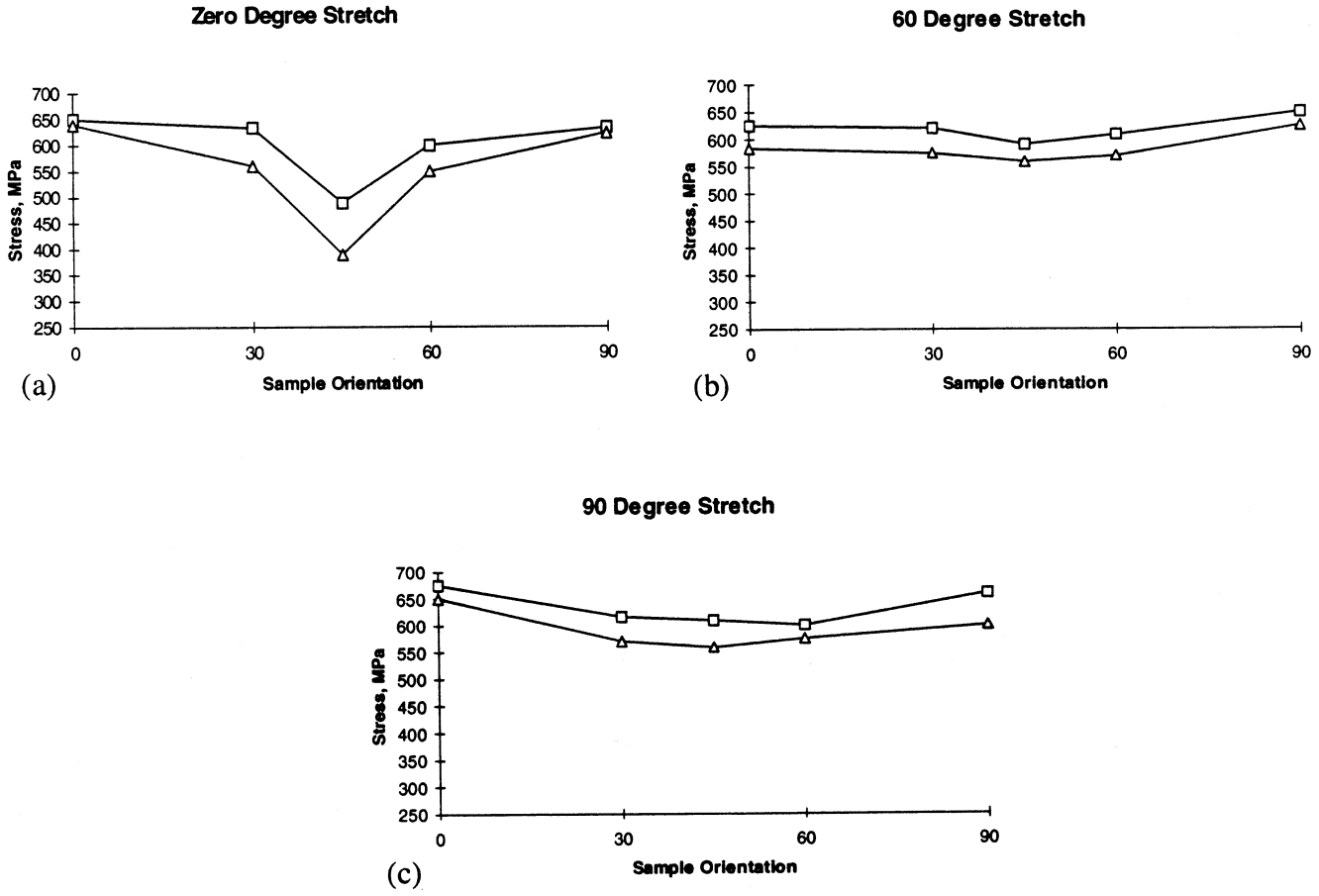

Fig. 10. Orientation dependence of tensile properties for alloy 2095. The upper curves are ultimate tensile strength and the lower curves are the yield strength at various tensile testing orientations.

showed evidence that slip can occur on {111}, {112}, {110} and {100} planes in aluminum alloys.

In order to determine the contribution of the crystallographic texture to the mechanical anisotropy, the experimental yield strength data was normalized by 'M' and the results were plotted in the graphs of Fig. 12. If crystallographic texture is the only factor affecting the yield strength, then the plot of Fig. 12 should fall on a straight line. The plot of the normalized yield strength based on restricted glide shows a convex shape and is nowhere close to a straight line. This suggests that crystallographic texture cannot be the only source of anisotropy. One possible reason for this anisotropy is the presence of the inhomogeneous distribution of T_1 precipitates on {111} planes. It must be noted that the {111} planes are also the slip planes in this material. Therefore, the glide dislocations will encounter a high resistance to move on some of the {111} slip plane, if the T_1 precipitates are inhomogeneously distributed as shown by Kim and Lee. [8]. More modeling effort is needed by considering the inhomogeneous distribution of T_1 precipitates to investigate the contribution to mechanical anisotropy. Another less likely explanation can be given based on the glide of dislocations on non-octahedral planes. Such a claim however requires more experimental evidence through Transmission Electron Microscope (TEM) analysis. The latter interpretation may be reinforced by considering the texture simulation performed by Bacroix and Jonas [26]. These researchers used non-octahedral slip on {110} and {112} planes, and predicted high Brass texture component in some hot rolled aluminum alloys. Incidentally, our texture results also show high Brass component (about 40 × random), and as such can be explained by Bacroix and Jonas model.

5. Conclusions

(1) Hot rolling of Al–Li 2095HT72 resulted in texture with very high Brass component (about 40 × random).

(2) Off-axis stretch followed by aging had little or no effect on the texture development of the solution heat treated material.

(3) Samples stretched at 0° until failure exhibited high mechanical anisotropy when the TA was 45°. The yield strength anisotropy for this condition was about 40%.

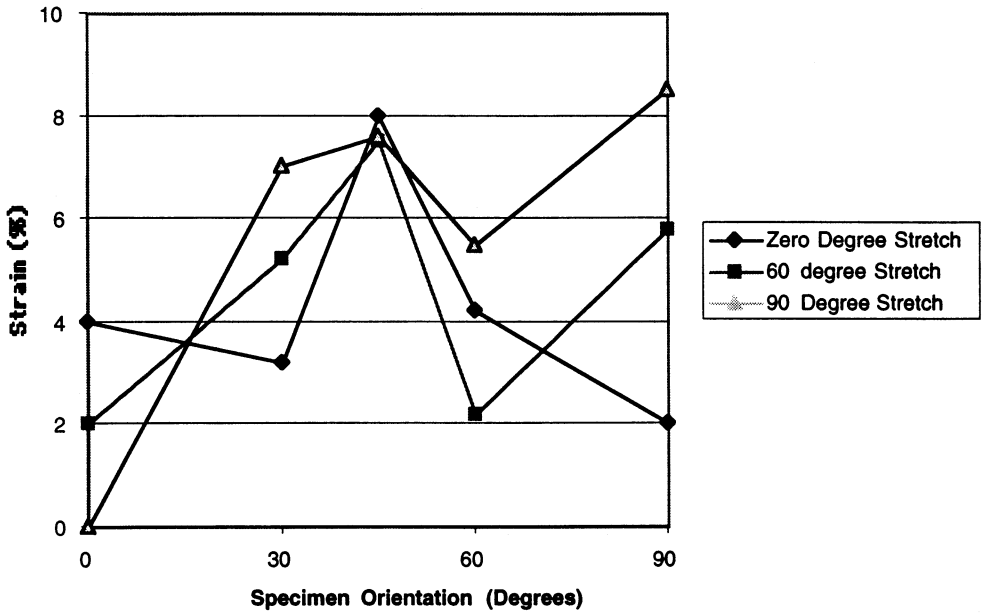

Fig. 11. The orientation dependence of the final elongation to failure for specimens initially stretched at 0°, 60° and 90° to the rolling direction.

(4) Significant reduction in mechanical anisotropy of 2095 Al–Li was achieved by employing off-axis stretching. Specimens with stretch axis of 60° and 90° orientations exhibited a yield strength anisotropy of about 10%.

(5) The yield strength data was normalized by the Taylor factor using the crystallographic texture data. The results showed that crystallographic texture was contributing only minimally to the apparent anisotropy. This may be justified by the inhomogeneous distribution of T_1 precipitates, which may inhibit glide on the primary slip systems.

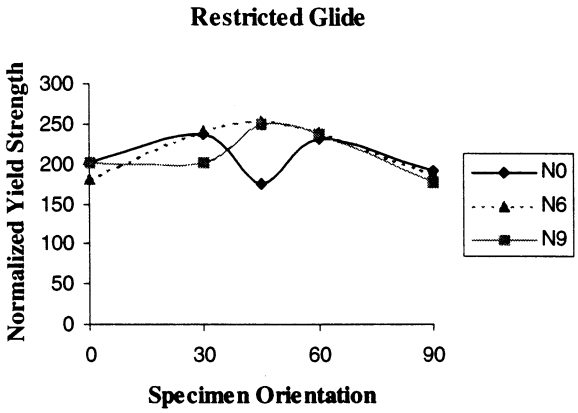

Fig. 12. Orientation dependence of normalized tensile properties (divided by Taylor factor) using the restricted glide approach. The simulation was performed for samples stretched and then aged at 180°C for 24 h.

Acknowledgements

The authors wish to thank the National High Magnetic Field Laboratory for laboratory facilities. One of the authors, L. Brandao would like to thank CAPES for partial funding provided.

Table 2
Taylor factors based on restricted glide approach

TA	Taylor Factor—RG			
	HT	S0	S6	S9
0	3.09	3.19	3.22	3.24
30	2.33	2.36	2.37	2.84
45	2.22	2.22	2.21	2.24
60	2.33	2.37	2.38	2.42
90	3.02	3.27	3.32	3.37

References

[1] W.S. Miller, J. White, D.J. Lloyd, The Metallurgy of Al–Li Based Alloys, in: E.A. Starke, J.T.H. Sanders (Eds.), Alluminum Alloys, Their Physical and Mechanical Properties, EMAS, University of Virginia, Charlottesville, VA, 1986.

[2] P.N. Kalu, Texture and recrystallization characteristics in Weldalite X2095 alloy plates. In: J.J. Jonas, T.R. Bieler, K.J. Bowman (Eds.), Advances in Hot Deformation and Microstructures. The Materials Society, 1994.

[3] P.J. Gregson, H.M. Flower, Acta Metall. 33 (1985) 527.

[4] S. Fox, H.M. Flower, D.S. McDarmaid, J.E.A. Starke, J.T.H. Sanders (Eds.), Alluminum Alloys—Their Physical and Mechanical Properties, EMAS, University of Virginia, Charlottesville, VA, 1986.

[5] O.S. Es-Said, E.W. Lee, The effect of stretch orientation (and rolling mode) on the tensile behavior of 2095 aluminum lithium alloy, in: E.W. Lee, N.V. Jata, W.E. Frazier (Eds.), Light Weight Alloys for Aerospace Applications III, TMS, Las Vegas, 1995.
[6] K. Lucke, J. Hirsch, O. Engler, T. Rickert, Rolling and recrystallization textures of Al alloys in presence of precipitation, in: J.E.A. Starke, J.T.H. Sanders Jr. (Eds.), Aluminum Alloys—Their Physical and Mechanical Properties, EMAS, University of Virginia, Charlottesville, VA, 1986.
[7] M. Peters, K. Welpmann, W. Zink, T.H. Sanders Jr., in: C. Baker, P.J. Gregson, S.J. Harris, C.J. Peel (Eds.), Fatigue Behavior of Al–Li–Cu–Mg Alloy, Institute of Metals, London, 1986, pp. 239–246.
[8] N.J. Kim, E.W. Lee, Acta Metall. Mater. 41 (1993) 941–948.
[9] D. Yao, D. Chu, J.W. Morris, Tensile deformation of Al–Cu–Li–Zr Alloy-2090-T8E41 at 298 and 77K, in: E.W. Lee, N.J. Kim (Eds.), Light-Weight Alloys for Aerospace Applications II, TMS, New Orleans, 1991.
[10] A.K. Vasudevan, Met. Trans. 19A (1988) 731.
[11] H.D. Chandler, J.N. Gortzen, Mater. Sci. Eng. A188 (1994) 97–102.
[12] E.W. Lee, W.E. Frazier, Scripta Metallurgica 22 (1988) 53–57.
[13] B. Nobel, G.E. Thompson, Met. Sci. J. 6 (1972) 167.
[14] R.A. Herring, F.W. Gayle, J.R. Pickens, J. Mater. Sci. 28 (1993) 69–73.
[15] A.K. Hardy, J.M. Silcock, J. Inst. Metals 84 (1955/56) 423.
[16] J. Martinez-Fernandez, et al., Acta Metall. Mater. 43 (1995) 2469–2484.
[17] J. Kallend, U.F. Kocks, A.D. Rollett, H.R. Wenk, Mater. Sci. Eng. A132 (1991) 1–11.
[18] A.K. Vasudevan, M.A. Przystupa, W.G.F. Jr., Scripta Metallurgica Materialia 24 (1990) 1429–1434.
[19] P. Regenet, H.P. Stuwe, Z. Metallkunde 54 (1963) 273.
[20] P.N. Kalu, L. Zhang, Scripta Materialia 39 (1998) 175–180.
[21] W. Truszkowski, J. Krol, B. Major, Metallurgical Trans. A 11A (1980) 749.
[22] E.W. Lee, J. Waldman, New Light Alloys, NATO, 1988.
[23] K.S. Kumar, S.A. Brown, J.R. Pickens, Acta Materialia 44 (1996) 1899–1915.
[24] K.S. Kumar, S.A. Brown, J.R. Pickens, Scripta Materialia 24 (1990) 1245–1250.
[25] C. Maurice, M.C. Theyssier, J.H. Briver, in: J.J. Jonas, K.J. Bowman (Eds.), Advances in Hot Deformation and Microstructures. The Minerals, Metals & Materials Society, 1994, pp. 411–425.
[26] B. Bacroix, J.J. Jonas, Textures Microstructures 8&9 (1988) 267–311.